DOI: 10.1002/chem.200700643

Design of Peptides That Form Amyloid-Like Fibrils Capturing Amyloid β1–42 Peptides

Junichi Sato, Tsuyoshi Takahashi, Hideo Oshima, Sachiko Matsumura, and Hisakazu Mihara*[a]

Abstract: Amyloid β-peptide (Aβ) plays a critical role in Alzheimer's disease (AD). The monomeric state of Aβ can self-assemble into oligomers, protofibrils, and amyloid fibrils. Since the fibrils and soluble oligomers are believed to be responsible for AD, the construction of molecules capable of capturing these species could prove valuable as a means of detecting these potentially toxic species and of providing information pertinent for designing drugs effective against AD. To this aim, we have designed short peptides with various hydrophobicities based on the sequence of Aβ14–23, which is a critical region for amyloid fibril formation. The binding of the designed peptides to Aβ and the amplification of the formation of peptide amyloid-like fibrils coassembled with Aβ are elucidated. A fluorescence assay utilizing thioflavin T, known to bind specifically to amyloid fibrils, revealed that two designed peptides (LF and VF, with the leucine and valine residues, respectively, in the hydrophobic core region) could form amyloid-like fibrils effectively by using mature Aβ1–42 fibrils as nuclei. Peptide LF also coassembled with soluble Aβ oligomers into peptide fibrils. Various analyses, including immunostaining with gold nanoparticles, enzyme-linked immunosorbent assays, and size-exclusion chromatography, confirmed that the LF and VF peptides formed amyloid-like fibrils by capturing and incorporating Aβ1–42 aggregates into their peptide fibrils. In this system, small amounts of mature Aβ1–42 fibrils or soluble oligomers could be transformed into peptide fibrils and detected by amplifying the amyloid-like fibrils with the designed peptides.

Keywords: Alzheimer's disease · amyloid β-peptide · amyloid fibrils · oligomers · peptide design

Introduction

The amyloid fibril formation of protein is related to fatal diseases.[1] Alzheimer's disease (AD) is a progressive neurodegenerative disease that is characterized by the abnormal accumulation of amyloid β-peptide (Aβ) in senile plaques.[2] Moreover, the pathogenesis of AD is closely related to the aging process.[3] Amyloid fibrils are believed to play a central role in the pathogenesis of AD since amyloid fibrils predominantly exist in senile plaques in the brains of patients with AD.[4] Aβ is produced by proteolysis of amyloid β precursor protein (APP) and is mostly composed of either 40 or 42 amino acids.[5]

Aβ spontaneously self-assembles into amyloid fibrils. Although the concentration of the 42 amino acid form (Aβ1–42) is approximately 10% that of the 40 amino acid form (Aβ1–40), Aβ1–42 is the predominant component of senile plaques.[6] Kinetic studies of Aβ have revealed that Aβ1–42 forms amyloid fibrils significantly faster than Aβ1–40.[6] On the other hand, recent studies suggest that soluble ligands such as Aβ oligomers might be the toxic species in amyloids.[7–10] Amyloid-derived diffusible ligands (ADDLs), composed of Aβ1–42, are potent neurotoxins that kill neurons in cultured hippocampal brain slices from mice at nanomolar concentrations.[7,8] Protofibrils and low-molecular-weight species of Aβ are also neurologically active.[9,10] Moreover, it has been reported that Aβ1–42 can form oligomeric aggregates more rapidly and stably than Aβ1–40.[11] Therefore, the construction of molecules capable of capturing Aβ1–42-generated amyloid fibrils and toxic oligomers is a potentially important approach for the characterization of the various aggregated species of Aβ and for developing a diagnostic methodology for AD.

[a] J. Sato, Dr. T. Takahashi, H. Oshima, Dr. S. Matsumura, Prof. H. Mihara
Graduate School of Bioscience and Biotechnology
Tokyo Institute of Technology
4259-B40, Nagatsuta, Yokohama (Japan)
Fax: (+81) 45-924-5833
E-mail: hmihara@bio.titech.ac.jp

Although structures of the soluble oligomers are not available, structural analyses of Aβ amyloid fibrils have been reported.[12,13] Tycko and co-workers reported that residues 1–10 are approximately disordered and that residues 12–24 and 30–40 form parallel β-sheet structures in the fibrils.[12] This model contains a bent structure and shows Asp23 and Lys28 making electrostatic interactions. Residues 11–25 are located in the central region of Aβ and are known to be important for fibril formation; the peptide Aβ11–25 has been found to form amyloid fibrils with morphology similar to that of full-length Aβ1–40 and Aβ1–42 fibrils.[14] The structure of this kind of fragment peptide has been analyzed by X-ray diffraction and solid-state NMR spectroscopy.[15–17] These data suggest that the peptide fibrils are composed of antiparallel β sheets in a cross-β arrangement and that the hydrophobic core (LVFFA) participates in an antiparallel β-sheet structure. The electrostatic interaction made by His14 and Asp23 might promote an antiparallel β-sheet structure in Aβ11–25. It was reported that the sequence including this hydrophobic core region could be utilized to design molecules that inhibit the fibrillization of Aβ.[18] These insights into the structural basis driving Aβ fibrillogenesis provide a foundation for the design of molecules that can coassemble with and capture Aβ fibrils and toxic oligomers.

In the present study, short peptides capable of forming amyloid-like fibrils containing an antiparallel β sheet were designed and synthesized. The peptides were designed by varying the hydrophobicity, with the expectation that different hydrophobicities would alter fibrillogenesis and binding to Aβ. If the designed peptide can form amyloid-like fibrils by using mature Aβ1–42 fibrils and Aβ1–42 soluble oligomers as nuclei, then these designed peptides can capture and amplify small amounts of Aβ fibrils and other toxic species of Aβ into stable and larger peptide fibrils. This unique property of the peptide ligands may be useful for the design of detection and diagnostic agents for AD.

Results and Discussion

Peptide design: Four peptides with the sequence Ac-KQKLL**X**FLEE-NH_2 (**X** = L, V, A, or T; peptides designated LF, VF, AF, and TF, respectively) were designed based on the structure of the core region of Aβ (amino acid residues 14–23; Figure 1). The cationic histidine and anionic aspartic acid residues of the Aβ14–23 were replaced by lysine and glutamic acid, respectively, to form favorable electrostatic interactions upon formation of the expected antiparallel structure.[16,17,19] It was predicted that variation in the hydrophobicity of the hydrophobic core region (LL**X**FL) could change the fibril-forming abilities of the designed peptides. The glutamine and phenylalanine residues were conserved due to their importance in fibril formation.[20] All of the designed peptides were synthesized by the 9-fluorenylmethoxycarbonyl (Fmoc) solid-phase method and identified by matrix-assisted laser-desorption/ionization time-of-flight mass spectrometry (MALDI-TOF MS).

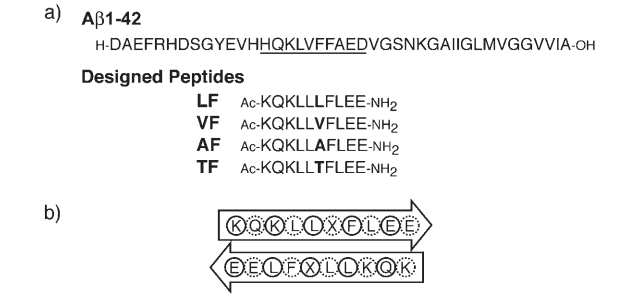

Figure 1. a) Sequences of Aβ1–42 and the designed peptides. The core sequence of Aβ for amyloid fibrils is underlined. b) Model for the antiparallel β-sheet structure of the designed peptides. The circled amino acids are the residues on the upper side of the strand, and those surrounded by dotted circles are the ones on the opposite side of the strand.

Structural and fibril-forming properties of the designed peptides: Circular dichroism (CD) spectra were measured to obtain information about the secondary structure of the designed peptides (100 μM) in 20 mM tris(hydroxymethyl)aminomethane–HCl (Tris-HCl) buffer (pH 7.4) containing 10% (v/v) trifluoroethanol (TFE); the CD spectra are shown in Figure 2. Small amounts of TFE (10–20% v/v) enhance the fibril formation of Aβ.[21] The LF and VF peptides showed typical β-sheet signals, with a negative minimum at 215 nm and a positive maximum at 200 nm. The intensity of the β-

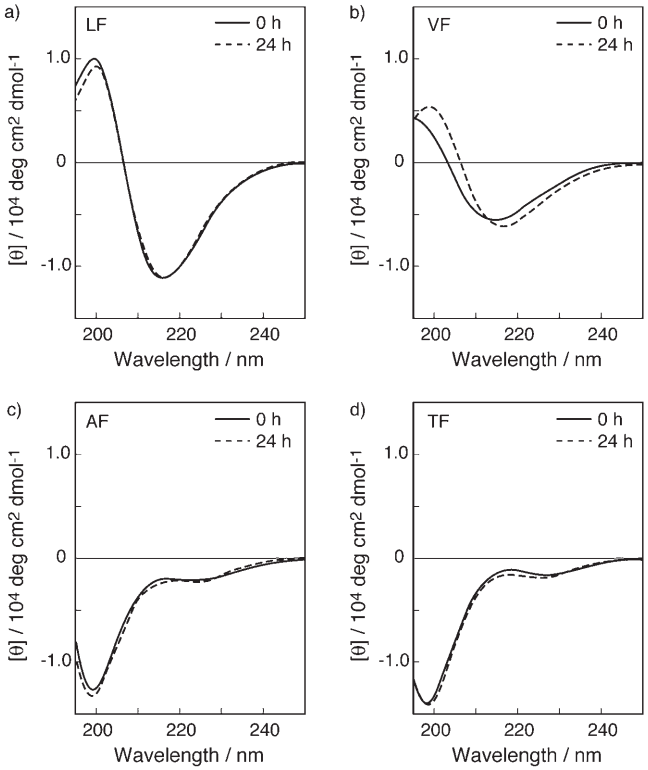

Figure 2. Circular dichroism spectra of the designed peptides. [peptide] = 100 μM in 20 mM Tris-HCl buffer (pH 7.4) containing 10% TFE at 25 °C. The CD spectra were measured just after preparation (——) and after 24 h of incubation at room temperature (-----)

sheet signal of the LF peptide was twofold stronger than that of the VF peptide. After 24 h at room temperature, the CD spectrum of the LF peptide did not change but the spectrum of the VF peptide showed a slightly enhanced β-sheet structure. By contrast, the AF and TF peptides showed CD signals typical of a random-coil structure, even after 24 h of incubation. The YF peptide, which has tyrosine at the **X** position, was also synthesized and provided results similar to those of AF and TF,[20] a result indicating that A, T, and Y inhibit the formation of stable β-sheet structures. These results suggest that the amino acid residue at position 6 in the hydrophobic core significantly affects the conformational properties of the designed peptides, and hydrophobic interactions between segments of the hydrophobic core are critical for the intermolecular assembly of β sheets in the peptides.

To evaluate the fibril-forming abilities of the designed peptides, each peptide (100 μM) was incubated in 20 mM Tris-HCl buffer (pH 7.4) containing 10% (v/v) TFE at room temperature. Fibril formation was monitored by using the thioflavin T (ThT) fluorescence assay (see the Experimental Section). ThT is known to bind to amyloid fibrils and emit a strong fluorescence near 485 nm after binding.[22] After incubation of LF in 10% TFE for 6 h, the fluorescence intensity of ThT increased significantly, a result suggesting amyloid-like fibril formation had occurred (Figure 3). ThT fluorescence in the presence of VF was slightly higher than that in the absence of the peptide. These results suggest that the LF and VF peptides have the potential to form amyloid-like fibrils. By contrast, the AF and TF peptides showed no changes in fluorescence, even after overnight incubation, thereby indicating that the AF and TF peptides cannot self-assemble into amyloid-like fibrils, possibly due to their low hydrophobicity. When the designed peptides were incubated in buffer containing 5% dimethylsulfoxide (DMSO) without

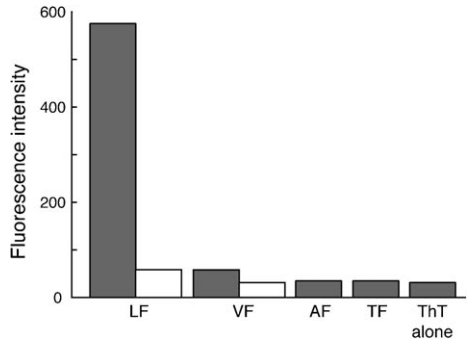

Figure 3. Fibrillogenesis of the designed peptides monitored by ThT fluorescence. The designed peptides (100 μM) were incubated for 6 h at room temperature in 20 mM Tris-HCl buffer (pH 7.4) containing 10% TFE (gray bars) and for 24 h in buffer containing 5% DMSO (white bars). The fluorescence of 6.3 μM ThT was measured with 5.0 μM peptides at 25 °C. $\lambda_{ex} = 440$ nm and $\lambda_{em} = 485$ nm.

TFE, the fluorescence intensity of ThT in the presence of LF after 24 h incubation was slightly higher that in the absence of peptide, but it did not change in the presence of the VF peptide. Stock solutions of the designed peptides were prepared in neat DMSO, so the peptides were essentially monomeric before the incubation in aqueous buffer, thus making it difficult for the peptides to form amyloid-like long fibrils in the absence of TFE.

TEM images of the designed peptides: To evaluate the features and morphologies of the LF and VF fibrils, transmission electron microscopy (TEM) images were obtained (Figure 4). The LF peptide (100 μM) incubated with 10% TFE generated long (several μm in length) tangled fibrils (Figure 4a), similar to mature Aβ fibrils. By contrast, the VF peptide (100 μM) incubated with 10% TFE formed short fibrils, pieces of which assembled into thick fibers (Fig-

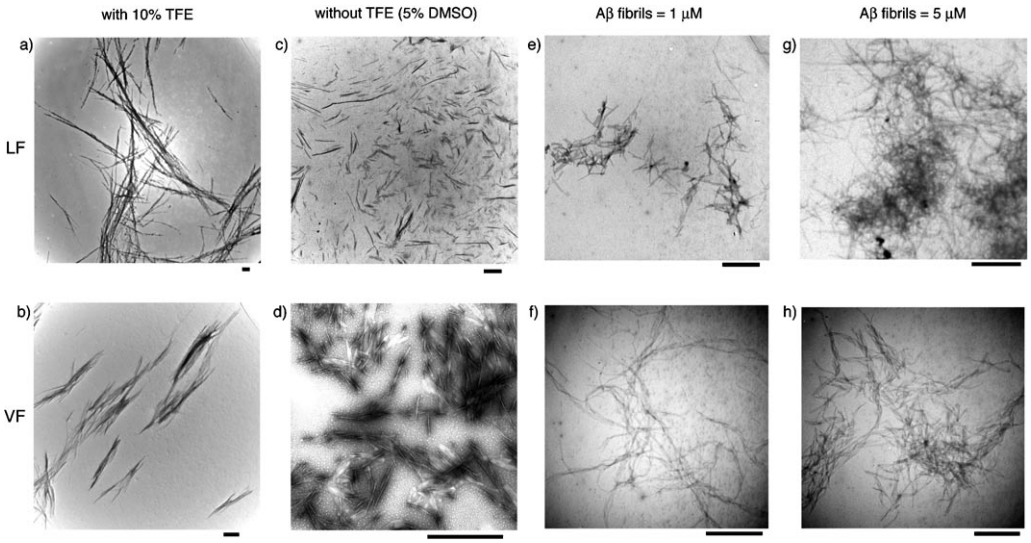

Figure 4. TEM images of the designed peptides LF (a, c, e, and g) and VF (b, d, f, and h) incubated with 10% TFE (a, b) and without TFE (c–h). The fibrils were prepared in the absence (a–d) and presence (e–h) of mature Aβ1–42 fibrils. Fibrils were stained with 2% uranyl acetate or 2% phosphotungstic acid. Scale bar = 1 μm.

ure 4b). Furthermore, the LF and VF fibrils formed in the absence of TFE, from DMSO stock, had short, flat-tape-like morphologies (0.2–1.5 μm in length; Figure 4c and d). These results suggest that the peptide sequence and incubation conditions alter the fibril morphology dramatically. These different morphologies might also change the affinity and fluorescence properties of ThT toward the fibrils: for example, the LF peptide in 10% TFE formed longer fibrils which bind to ThT, thereby enhancing the ThT fluorescence significantly, while the same peptide in 5% DMSO formed shorter fibrils which cannot enhance ThT fluorescence.

Fibril formation of designed peptides with mature Aβ1–42 fibrils: To evaluate the ability of the designed peptides to form fibrils with mature Aβ1–42 fibrils, the LF and VF peptides (100 μM each) were incubated either with a small amount of Aβ1–42 fibrils (1, 5, and 10 μM) or in the absence of Aβ; all incubations took place in 20 mM Tris-HCl buffer (pH 7.4) containing 5% (v/v) DMSO. The ThT fluorescence was measured before and after 8 h of incubation of the peptides with or without the Aβ fibrils. The fluorescence intensities of ThT in the presence of the LF and VF peptides were significantly increased by incubation with Aβ fibrils (Figure 5), and the fluorescence intensity of LF with Aβ fibrils was higher than that of VF with Aβ fibrils. Furthermore, the fluorescence increase was dependent on the increase in the amount of Aβ1–42 fibrils. No fluorescence change was observed with mature Aβ1–42 fibrils (10 μM) alone (data not shown). These results suggest that the LF and VF peptides can form amyloid-like fibrils by using Aβ1–42 fibrils as nuclei, although the peptides alone did not form ThT-sensitive fibrils in the absence of TFE (DMSO stock). LF and VF presumably interact with the Aβ1–42 fibrils due to the sequence similarity of their hydrophobic cores, and these interactions effectively promote fibrillogenesis of the LF and VF peptides. LF alone has a higher propensity to self-assemble than VF and this leads to easier fibril formation with Aβ1–42 fibrils. Thus, formation of the Aβ-like fibrils was accelerated and fibrils were accumulated by the designed peptides LF and VF. A small amount of Aβ1–42 fibrils could be detected by amplification of the peptide fibrils.

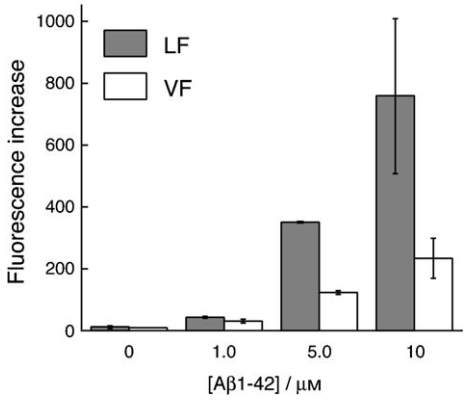

Figure 5. Fluorescence increase of ThT before and after 8 h of incubation of the LF (gray bars) and VF (white bars) peptides (100 μM) with and without mature Aβ1–42 fibrils (0, 1, 5, 10 μM per monomer) at 37°C. The fluorescence of 6.3 μM ThT was measured with 5.0 μM peptides at 25°C. $\lambda_{ex}=435$ nm and $\lambda_{em}=485$ nm.

TEM images of the designed peptides with Aβ1–42 fibrils: TEM images of the LF and VF peptides with mature Aβ1–42 fibrils were obtained (Figure 4e–h). When either LF or VF was incubated with Aβ fibrils, long tangled fibrils (amyloid-like fibrils) were clearly observed. Furthermore, the amount of fibrils on the TEM grid increased with increasing Aβ concentrations, and fewer fibrils were formed in the absence of LF and VF. These results, confirmed by ThT fluorescence analyses (Figure 5), suggest that the Aβ1–42 fibrils assist LF and VF in forming amyloid-like fibrils by acting as templates.

To confirm whether the Aβ1–42 fibrils were absorbed into amyloid-like fibrils composed of the designed peptides, immunostaining by using the 6E10 anti-Aβ antibody, which recognizes the N terminal of Aβ (residues 1–16), conjugated with biotin (biotin–6E10) and gold nanoparticles (10 nm diameter) conjugated with the antibiotin antibody was carried out on a TEM grid (Figure 6). Although the gold nanoparticles could not be observed in the LF or VF peptide fibrils alone, the gold particles were observed in significant amounts on fibrils of LF or VF mixed with a small amount of Aβ. Furthermore, the gold particles on the peptide fibrils increased with increasing Aβ concentrations, a result indicating that the Aβ1–42 fibrils can be captured and coassembled with the peptide fibrils.

Fibril formation of designed peptides with Aβ1–42 oligomers: It has been reported that Aβ1–42 readily aggregates into metastable oligomers at near physiological concentrations (1–20 nM)[23] and that these soluble oligomers might be the toxic species of amyloids.[7–10] We therefore evaluated whether the designed peptides could form amyloid-like fibrils by capturing the Aβ1–42 soluble oligomers. To generate the Aβ1–42 oligomers, Aβ1–42 treated with 1,1,1,3,3,3-hexafluoro-2-propanol (HFIP; see the Experimental Section) was incubated in Dulbecco's phosphate-buffered saline (PBS) for 1 day at room temperature. The oligomers were detected by size-exclusion chromatography (SEC). The peak near the void volume consisted of Aβ1–42 oligomers (see Figure 8b); TEM images of the oligomers are shown in Figure 7a.

The LF and VF peptides (100 μM) were individually incubated with the Aβ1–42 oligomers in the Dulbecco's PBS at 37°C, and fibril formation by the peptides was examined by using the ThT binding assay. The fluorescence intensity of ThT in the presence of the LF peptide was significantly increased by incubation with the Aβ oligomers in a concentration-dependent manner (Figure 7b), similar to the result obtained by incubation with mature Aβ1–42 fibrils (Figure 5). By contrast, ThT fluorescence in the presence of VF was

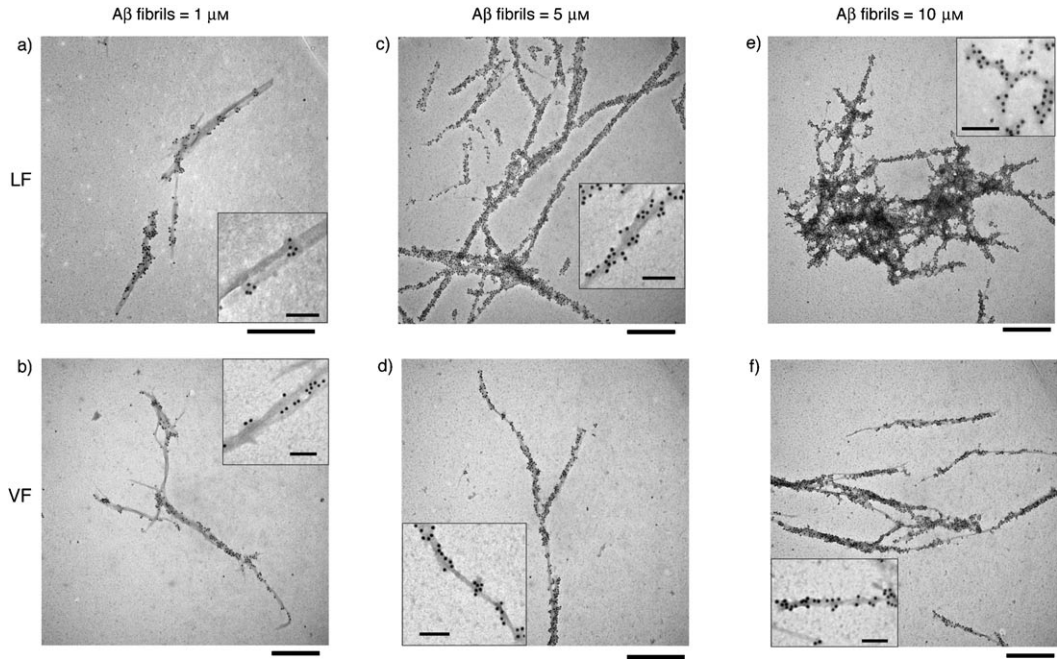

Figure 6. Immunostained TEM images of LF (a, c, and e) and VF (b, d, and f) incubated with mature Aβ1–42 fibrils. The concentrations of Aβ1–42 were 1 (a, c), 5 (c, d), and 10 μM (e, f). The Aβ1–42 species on the fibrils were immunostained with antibody-conjugated gold nanoparticles. Fibrils were stained with 2% uranyl acetate. Scale bar = 500 nm (inset = 100 nm).

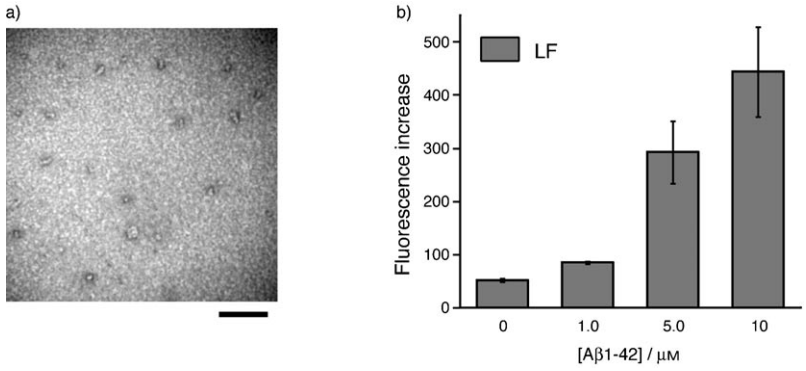

Figure 7. a) TEM image of Aβ1–42 large oligomers. Scale bar = 100 nm. b) Fluorescence increase of ThT before and after 8 h of incubation of the designed peptides (100 μM) with and without Aβ1–42 soluble oligomers (0, 1, 5, and 10 μM) at 37 °C. The fluorescence of 6.3 μM ThT was measured with 5.0 μM peptides at 25 °C. $\lambda_{ex} = 435$ nm and $\lambda_{em} = 485$ nm.

not obviously increased by incubation with the Aβ oligomers. The VF peptide alone showed a lower ability to form amyloid-like fibrils than the LF peptide alone, as shown in Figure 3. Therefore, the ability of the peptide to form fibrils is related to the fibril formation with Aβ oligomers as nuclei.

When the LF peptide forms amyloid-like fibrils with Aβ oligomers, the Aβ oligomers can be captured in the LF fibrils. To evaluate whether the soluble Aβ oligomers coassemble, an enzyme-linked immunosorbent assay (ELISA) with a fluorogenic peroxidase substrate for detecting Aβ oligomers was carried out by using the supernatant after the fibrils were removed by centrifugation (Figure 8a). It has been reported that Aβ oligomers can be detected by using capture and detection antibodies (6E10 and biotin–6E10, respectively) capable of recognizing the same primary sequence epitope.[23] Nanomolar-level oligomerization can be detected easily, but monomeric Aβ, with a single epitope, cannot be detected. By using this sandwich ELISA with 6E10 and biotin–6E10, Aβ oligomers in the supernatant were detected at a higher level in the absence of LF. In a sample immediately after mixing with LF, however, the fluorescence signal in the ELISA was much lower than that in the absence of LF. Furthermore, Aβ oligomers in the supernatant of a sample after 2 h of incubation were hardly detectable above background level. SEC analysis also confirmed that samples after incubation with LF contained a smaller amount of Aβ oligomers than samples before incubation with LF (Figure 8b). These results strongly suggest that the LF peptide captures soluble Aβ oligomers effectively in its amyloid-like fibrils.

TEM images of the LF peptide incubated with Aβ oligomers: To confirm whether Aβ1–42 oligomers were captured

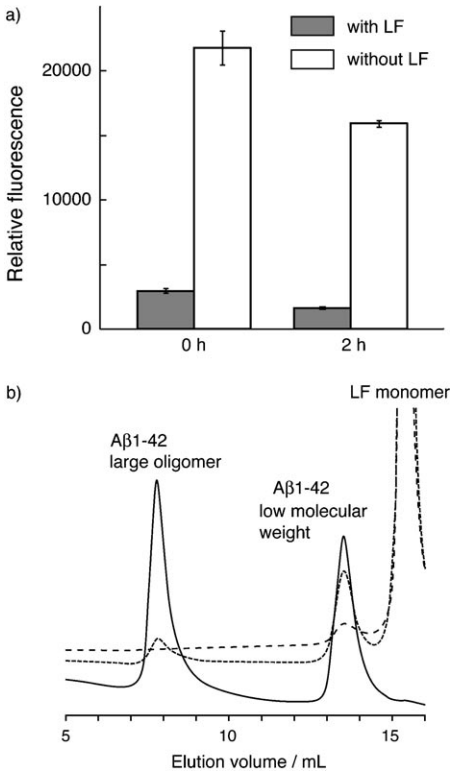

Figure 8. a) ELISA assay for Aβ1–42 soluble oligomers by using anti-Aβ 6E10 (capture) and biotinylated 6E10 (detection) antibodies. The supernatants were measured after centrifugation of the Aβ1–42 oligomers incubated with (gray bars) or without (white bars) LF. b) SEC analysis of the supernatants after centrifugation before (——) and after incubation with LF (0 h, •••••; 2 h, -----) on a Superdex 75 column.

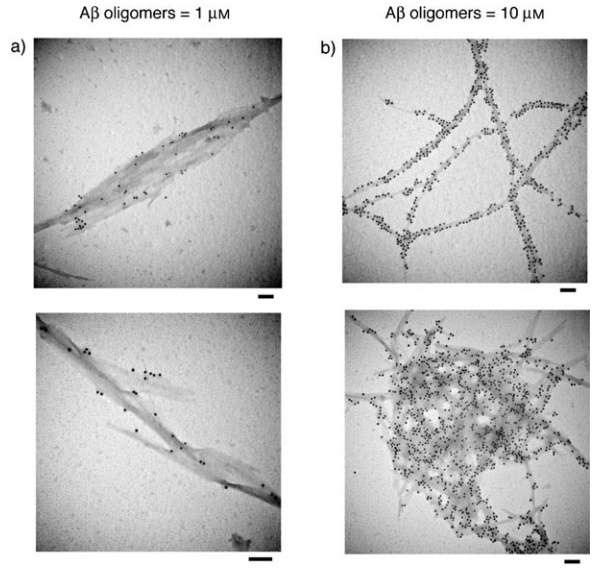

Figure 9. Immunostained TEM images of LF fibrils incubated with Aβ1–42 soluble oligomers. The concentrations of Aβ1–42 were a) 1 and b) 10 μM. The Aβ1–42 species on the fibrils were immunostained with antibody-conjugated gold nanoparticles. Fibrils were stained with 2% uranyl acetate. Scale bar = 100 nm. Two images are shown for each set of conditions.

and coassembled into the amyloid-like fibrils composed of the LF peptide, immunostaining analysis with gold nanoparticles was carried out on a TEM grid (Figure 9). Gold nanoparticles were observed on LF fibrils incubated with Aβ1–42 oligomers. The number of gold particles on the fibrils increased with increasing Aβ1–42 oligomer concentration, similar to the result obtained with mature Aβ1–42 fibrils. The nanoparticles on the oligomer–peptide fibrils were more uniformly distributed than those on LF fibrils with mature Aβ1–42 fibrils. Since the size of the gold particles (10 nm diameter) is similar to that of the large Aβ1–42 oligomers, one gold particle could bind to one Aβ oligomer; therefore, the particles might be observed separately and not assembled on the LF fibrils. Furthermore, gold particles cannot be observed on LF fibrils alone. These results confirm that the Aβ1–42 oligomers can be captured by the LF fibrils.

Discussion

Short peptides capable of forming amyloid-like fibrils by capturing Aβ1–42 fibrils and soluble oligomers have been designed and synthesized. The LF and VF peptides incubated without TFE or Aβ formed short flat fibrils. ThT, a specific binder to amyloid fibrils, cannot react with such LF and VF fibrils (DMSO stock). By contrast, the LF and VF peptides incubated with mature Aβ1–42 fibrils formed amyloid-like fibrils to which ThT bound. The different morphologies and ThT-binding properties of the peptide fibrils with and without the Aβ1–42 fibrils indicate that the LF and VF peptides interact with the Aβ1–42 fibrils and form amyloid-like fibrils. Furthermore, a TEM study with gold nanoparticles also revealed that LF and VF coassembled with the Aβ1–42 fibrils. In this system, small amounts of mature Aβ1–42 fibrils were detected by amplification of the Aβ fibrils as amyloid-like fibrils composed of LF or VF.

In the case of the Aβ1–42 soluble oligomers (which are believed to be the more toxic species), the LF, but not the VF, peptide can bind to the soluble oligomers immediately and form amyloid-like fibrils. The Aβ1–42 soluble oligomers captured by the LF fibrils can be removed easily by centrifugation. VF cannot capture the Aβ1–42 oligomers effectively. The VF peptide forms amyloid-like fibrils in Tris-HCl buffer without NaCl but hardly form fibrils in phosphate-buffered saline. The LF peptide rapidly self-assembles and can capture Aβ1–42 soluble oligomers into LF fibrils. Thus, the soluble oligomers can be detected by amplification into stable peptide fibrils. The construction of capturing agents for amyloid fibrils and toxic oligomers of Aβ1–42 is useful for characterization of the various species of Aβ aggregates and for developing detection and diagnostic agents for AD. In particular, since the soluble oligomers can be trapped into the peptide fibrils, the LF peptide might transform the toxic Aβ1–42 oligomers into less toxic species. Evaluation of

the biological activity of the designed fibrils is currently underway.

Experimental Section

Chemicals and reagents: All chemicals and solvents were of reagent or HPLC grade. Amino acid derivatives and reagents for peptide synthesis were purchased from Watanabe Chemical (Hiroshima, Japan). MALDI-TOF MS was performed on a Shimadzu MALDI III mass spectrometer by using 3,5-dimethoxy-4-hydroxycinnamic acid as a matrix. HPLC was carried out on a YMC ODS A-302 5C18 column (4.6×150 mm; YMC, Tokyo, Japan), a YMC ODS A-323 5C18 column (10×250 mm), or Develosil packed ODS-UG-5 columns (4.6×150 mm, 10×250 mm) by employing a Hitachi L-7000 HPLC system. Amino acid analyses were performed by using the phenyl isothiocyanate (PTC) method on a Wakopak WS-PTC column (Wako chemical, Osaka Japan). 6E10 antibody and biotinylated 6E10 were purchased from Signet Laboratories (Dedham, MA, USA). Electron microscopy was performed with a H-7500 electron microscope at 80 or 100 kV (Hitachi High-technologies, Tokyo, Japan). Streptavidin-conjugated horseradish peroxidase was purchased from Amersham Bioscience (Tokyo, Japan). QuantaBlu, a fluorescent substrate for peroxidase, was purchased from Pierce Biotechnology (Rockford, IL, USA). High-binding 96-well plates for the ELISA were purchased from Corning (Tokyo, Japan).

Peptide synthesis: The peptides, both the designed ones and Aβ1–42, were synthesized by the solid-phase method by using the Fmoc strategy with *O*-(7-azabenzotriazole-1-yl)-1,1,3,3-tetramethyluronium hexafluorophosphate (HATU) or 2-(1*H*-benzotriazole-1-yl)-1,1,3,3-tetramethyluronium hexafluorophosphate (HBTU) and 1-hydroxybenzotriazole hydrate ($HOBt{\cdot}H_2O$) as the coupling reagents. To remove the resin and the protecting groups, the peptide resin was treated with trifluoroacetic acid (TFA) containing *m*-cresol, ethanedithiol, and thioanisole as scavengers for 1 h at room temperature. The product was solidified with diethyl ether in an ice bath. The designed peptides were purified with reversed-phase (RP) HPLC on the YMC ODS A-323 column by using a linear gradient of acetonitrile/0.1% TFA to give the purified peptides. Aβ1–42 was purified with RP HPLC on the Develosil packed ODS-UG-5 column by using a linear gradient of acetonitrile/0.1% NH_4OH. Peptides were identified by their molecular ion peak $[M+H]^+$ in the MALDI-TOF mass spectrum: *m*/*z* found (calcd): LF: 1302.9 (1302.6); VF: 1287.1 (1288.6); AF: 1259.4 (1260.5); TF: 1352.0 (1352.6); Aβ1–42: 4518.0 (4515.1).

Sample preparation: The peptide stock solution was prepared in neat TFE or DMSO at a concentration of 1 mM or 2 mM, respectively. The peptide concentration was determined by quantitative amino acid analysis. Peptides were diluted in 20 mM Tris-HCl buffer (pH 7.4) or Dulbecco's PBS (0.7 mM KCl, 0.4 mM KH_2PO_4, 137 mM NaCl, 8.1 mM Na_2HPO_4, pH 7.5) with or without Aβ1–42 to start the incubation. Aβ1–42 was dissolved in HFIP to monomerize, and then the solution was evaporated. The monomerized Aβ1–42 was dissolved in dimethylsulfoxide, and then a buffer solution was added to start the incubation (final DMSO concentration: 4%). Mature Aβ1–42 fibrils were prepared by incubation of 100 μM Aβ1–42 in 20 mM Tris-HCl buffer for 1 week at room temperature. Before the mature Aβ1–42 fibrils were used, they were sonicated to make a homogeneous solution. Aβ1–42 soluble oligomers were prepared by incubation of 40 μM Aβ1–42 in Dulbecco's PBS for 24 h and centrifugation (18800 *g*, 60 min) to remove the larger aggregates such as fibrils.

Circular dichroism measurement: CD measurements were performed on a Jasco J-720WI spectropolarimeter equipped with a thermoregulator and with a quartz cell with a 1.0-mm path length. Spectra were recorded in terms of mean residue ellipticity (θ, in $deg\,cm^2\,dmol^{-1}$). A stock solution of each peptide in TFE was diluted in 20 mM Tris-HCl buffer (pH 7.4). The final concentration of the peptides was 100 μM in the buffer containing 10% (v/v) TFE. The concentration of the peptide solutions was determined by quantitative amino acid analysis.

Thioflavin T fluorescence analysis: ThT (Aldrich Chemical Co.) was dissolved at a cocentration of 250 μM in water. The ThT stock solution (10 μL) was added to the peptide solution (390 μL; the final concentrations of ThT and the peptide were 6.3 and 5 μM, respectively), and then fluorescence emission spectra were recorded immediately at an excitation wavelength of 440 nm at 25°C. Fluorescence spectra were measured on a Hitachi F2500 fluorescence spectrophotometer by using a 5×5 mm quartz cell.

Transmission electron microscopy: The peptide solution (10 μL) was absorbed on to a carbon-coated copper grid (200 mesh) by floating the grid on a drop of the peptide solution for 30–60 s. The excess solution was removed by filter-paper blotting, the grid was washed by floating on a drop of water for 10 s, and then the water was removed. The sample on the grid was then negatively stained with a 2% (w/v) aqueous phosphotungstic acid or uranyl acetate solution for 30 s and the excess staining solution was removed. After drying, the samples were visualized with a Hitachi H-7500 electron microscope operating at 80 or 100 kV.

To detect the Aβ1–42 on the peptide fibrils, biotinylated anti-Aβ antibodies (biotin–6E10) and antibiotin antibody-conjugated gold nanoparticles were used. The peptide solution (10 μL) was absorbed on to a carbon-coated copper grid (200 mesh) by floating the grid on a drop of the peptide solution for 30–60 s. The excess solution was removed with filter paper, and the grid was blocked by 20 mM Tris-HCl buffer (10 μL) containing 150 mM NaCl and 0.05% (v/v) Tween 20 (TBST) with 1% (w/v) bovine serum albumin (BSA) for 15 min. The grid was washed with TBST (10 μL×2), and then the peptide fibrils on the grid were treated with biotin–6E10 (10 $\mu g\,mL^{-1}$) in TBST with 1% BSA (10 μL) for 30 min. The grid was washed with TBST (10 μL×3), and then fibrils on the grid were treated with 1% (v/v) antibiotin antibody-conjugated gold nanoparticle solution in TBST with 1% BSA (10 μL) for 30 min. The grid was washed with TBST (10 μL×3) and water (10 μL×1), and then the grid was stained by 2% (w/v) uranyl acetate aqueous solution for 1–2 min. After drying, the samples were visualized with a Hitachi H-7500 electron microscope operating at 80 kV.

ELISA: To detect the Aβ1–42 oligomers, an ELISA was carried out. The 6E10 antibody (2 μg per well) was coated on a 96-well high-binding plate at 4°C overnight. The wells were blocked by TBST with 1% BSA (200 μL) at room temperature for 90 min. The wells were washed with TBST (200 μL×3). The samples were centrifuged at 18800 *g* for 60 min at 4°C to remove fibrils. The resulting supernatants were diluted 100-fold into TBST, and then the solution (100 μL) was added into the wells for 30 min at 4°C. The wells were washed with TBST (200 μL×3), biotin–6E10 (1 $\mu g\,mL^{-1}$) in TBST with 1% BSA (100 μL) was added, and the mixture was incubated for 90 min at room temperature. The wells were washed with TBST (200 μL×3), and then streptavidin-conjugated horseradish peroxidase (1 $\mu g\,mL^{-1}$) in TBST with 1% BSA (100 μL) was added and incubated for 30 min at room temperature. The wells were washed with TBST (200 μL×3), and then QuantaBlu fluorogenic peroxidase substrate (Pierce, 100 μL) was added and incubated for 60 min. The stop solution (Pierce, 100 μL) was added and the fluorescence was measured on a Twinkle LB970 fluorometer. An excitation filter of 355 nm (bandwidth ± 20 nm) and an emission filter of 460 nm (bandwidth ± 12.5 nm) were used.

Size-exclusion chromatography: For analytical size-exclusion chromatography, a Superdex 75 10/300 GL column (10×300 mm) (Amersham Bioscience) was used with Dulbecco's PBS as the eluent at a flow rate of 0.4 $mL\,min^{-1}$. To detect the Aβ1–42 soluble oligomers, the samples were centrifuged at 18800 *g* for 60 min at 4°C. The resulting supernatant was injected into the column and detected by absorbance at 220 nm on an HPLC system. The following proteins were used as molecular-weight standards: BSA (66 kDa), carbonic anhydrase (29 kDa), cytochrome *c* (12.4 kDa), aprotinin (6.5 kDa), and insulin B chain (3.5 kDa).

Acknowledgements

This work was supported in part by a Grant-in-Aid for Scientific Research from the Ministry of Education, Science, Culture and Sports, Japan.

[1] M. E. Huff, W. E. Balch, J. W. Kelly, *Curr. Opin. Struct. Biol.* **2003**, *13*, 674–682.
[2] D. J. Selkoe, *Nat. Cell Biol.* **2004**, *6*, 1054–1068.
[3] E. Cohen, J. Bieschke, R. M. Perciavalle, J. W. Kelly, A. Dillin, *Science* **2006**, *313*, 1604–1610.
[4] J. Hardy, *Trends Neurosci.* **1997**, *20*, 154–159.
[5] N. Suzuki, T. T. Cheung, X. D. Cai, A. Odaka, L. Otvos, C. Eckman, T. E. Golde, S. G. Younkin, *Science* **1994**, *264*, 1336–1340.
[6] J. T. Jarrett, E. P. Berger, P. T. Lansbury, *Biochemistry* **1993**, *32*, 4693–4697.
[7] R. W. Hepler, K. M. Grimm, D. D. Nahas, R. Breese, E. C. Dodson, P. Acton, P. M. Keller, M. Yeager, H. Wang, P. Shughrue, G. Kinney, J. G. Joyce, *Biochemistry* **2006**, *45*, 15157–15167.
[8] M. P. Lambert, A. K. Barlow, B. A. Chromy, C. Edwards, R. Freed, M. Liosatos, T. E. Morgan, I. Rozovsky, B. Trommer, K. L. Viola, P. Wals, C. Zhang, C. E. Finch, G. A. Krafft, W. L. Klein, *Proc. Natl. Acad. Sci. USA* **1998**, *95*, 6448–6453.
[9] S. Lesné, M. T. Koh, L. Kotilinek, R. Kayed, C. G. Glabe, A. Yang, M. Gallagher, K. H. Ashe, *Nature* **2006**, *440*, 352–357.
[10] D. M. Hartley, D. M. Walsh, C. P. Ye, T. Diehl, S. Vasquez, P. M. Vassilev, D. B. Teplow, D. J. Selkoe, *J. Neurosci.* **1999**, *19*, 8876–8884.
[11] G. Bitan, M. Kirkitadze, A. Lomakin, S. S. Vollers, G. B. Benedek, D. B. Teplow, *Proc. Natl. Acad. Sci. USA* **2003**, *100*, 330–335.
[12] a) A. T. Petkova, W.-M. Yau, R. Tycko, *Biochemistry* **2006**, *45*, 498–512; b) A. T. Petkova, Y. Ishii, J. J. Balbach, O. N. Antzutkin, R. D. Leapman, F. Delaglio, R. Tycko, *Proc. Natl. Acad. Sci. USA* **2002**, *99*, 16742–16747.
[13] T. Lührs, C. Ritter, M. Adrian, D. Riek-Loher, B. Bohrmann, H. Döbeli, D. Schubert, R. Riek, *Proc. Natl. Acad. Sci. USA* **2005**, *102*, 17342–17347.
[14] L. C. Serpell, J. M. Smith, *J. Mol. Biol.* **2000**, *299*, 225–231.
[15] L. C. Serpell, C. C. F. Blake, P. E. Fraser, *Biochemistry* **2000**, *39*, 13269–13275.
[16] A. Petkova, G. Buntkowsky, F. Dyda, R. D. Leapman, W.-M. Yau, R. Tycko, *J. Mol. Biol.* **2004**, *335*, 247–260.
[17] P. Sikorski, E. D. T. Atkins, L. C. Serpell, *Structure* **2003**, *11*, 915–926.
[18] a) M. A. Findels, G. M. Musso, C. C. Arico-Muendel, H. W. Benjamin, A. M. Hundal, J.-J. Lee, J. Chin, M. Kelley, J. Wakefield, N. J. Hayward, S. M. Molineaux, *Biochemistry* **1999**, *38*, 6791–6800; b) C. Soto, M. S. Kindy, M. Baumann, B. Frangione, *Biochem. Biophys. Res. Commun.* **1996**, *226*, 672–680; c) R. J. Chalifour, R. W. McLaughlin, L. Lavoie, C. Morissette, N. Tremblay, M. Boulé, P. Sarazin, D. Stéa, D. Lacombe, P. Tremblay, *J. Biol. Chem.* **2003**, *278*, 34874–34881; d) L. O. Tjernberg, J. Näslund, F. Lindqvist, J. Johansson, A. R. Karlström, J. Thyberg, L. Terenius, C. Nordstedt, *J. Biol. Chem.* **1996**, *271*, 8545–8548.
[19] Y. Takahashi, A. Ueno, H. Mihara, *ChemBioChem* **2002**, *3*, 637–642.
[20] T. Takahashi, H. Mihara, unpublished results.
[21] Y. Fezoui, D. B. Teplow, *J. Biol. Chem.* **2002**, *277*, 36948–36954.
[22] H. LeVine, *Protein Sci.* **1993**, *2*, 404–410.
[23] H. LeVine, *Anal. Biochem.* **2004**, *335*, 81–90.

Received: April 27, 2007
Published online: July 2, 2007

